the plant journal

SEB Society for Experimental Biology

The Plant Journal (2018) **96,** 801–814 doi: 10.1111/tpj.14069

Daily heliotropic movements assist gas exchange and productive responses in DREB1A soybean plants under drought stress in the greenhouse

Miroslava Rakocevic[1,2,*], Mariele Müller[3], Fabio Takeshi Matsunaga[4], Norman Neumaier[5], José Renato Bouças Farias[5], Alexandre Lima Nepomuceno[5] and Renata Fuganti-Pagliarini[5]

[1]*Embrapa Agricultural Informatics, Av. André Tosello 209, PO Box 6041, 13083-886 Campinas, São Paulo, Brazil,*

[2]*Department of Plant Biology Institute of Biology, University of Campinas – UNICAMP, R. Monteiro Lobato, 255, Cidade Universitária, 13083-862 Campinas, São Paulo, Brazil,*

[3]*University of Passo Fundo, BR 285 Km 292, 99052-900 Passo Fundo, Rio Grande do Sul, Brazil,*

[4]*Federal University of Technology of Paraná – UTFPR, Av. Alberto Carazzai, 1640, 86300-000 Cornélio Procópio, Paraná, Brazil, and*

[5]*Embrapa Soybean, Rodovia Carlos João Strass, Distrito de Warta, 86001-970 Londrina, Paraná, Brazil*

Received 24 April 2018; revised 18 July 2018; accepted 13 August 2018; published online 17 August 2018.
*For correspondence (e-mail mimarako@unicamp.br)

SUMMARY

Drought stress is one of the most severe environmental constraints on plant production. Under environmental pressures, complex daily heliotropic adjustments of leaflet angles in soybean can help to reduce transpiration losses by diminishing light interception (paraheliotropism), increase diurnal carbon gain in sparse canopies and reduce carbon gain in dense canopies by solar tracking (diaheliotropism). The plant materials studied were cultivar BR 16 and its genetically engineered isoline P58, ectopically overexpressing AtDREB1A, which is involved in abiotic stress responses. We aimed to follow the movements of central and lateral leaflets in vegetative stages V7–V10 and reproductive stages R4–R5, integrating the reversible morphogenetic changes into an estimate of daily plant photosynthesis using three-dimensional modeling, and to analyze the production parameters of BR 16 and P58. The patterns of daily movements of central leaflets of BR 16 in V7–V10 and R4–R5 were similar, expressing fewer diaheliotropic movements under drought stress than under non-limiting water conditions. Daily heliotropic patterns of lateral leaflets in V7–V10 and R4–R5 showed more diaheliotropic movements in drought-stressed P58 plants than in those grown under non-limiting water conditions. Leaf area in R4–R5 was generally higher in P58 than in BR 16. Drought significantly affected gas exchange and vegetative and reproductive architectural features. DREB1A could be involved in various responses to drought stress. Compared with the parental BR 16, P58 copes with drought through better compensation between diaheliotropic and paraheliotropic movements, finer tuning of water-use efficiency, a lower transpiration rate, higher leaf area and higher pod abortion to accomplish the maximum possible grain production under continued drought conditions.

Keywords: diaheliotropic, DREB1A, drought, leaf area, paraheliotropic, photosynthesis, pod production, stomatal conductance, transpiration, water-use efficiency.

INTRODUCTION

Lack of water is an environmental factor that strongly limits agricultural production worldwide. Agricultural drought is a condition in which the amount of water available through rainfall and/or irrigation and/or retained by the soil is insufficient to meet the transpiration needs of the crop (Tuberosa, 2012). The land area under vegetation suffering from drought will increase due to global warming (Cook *et al.*, 2014) and more than half the world's population will suffer acute water shortages by 2050 (Gobarah *et al.*, 2015). Improving plant yield under drought is a great challenge for plant breeding programs, with criteria generally focused on transpiration efficiency, early flowering and early vegetative area development (Richards, 1996).

The first criterion for the improvement of plant yield under drought is a high water-use efficiency (WUE) (Richards, 1996). Stomatal control of gas exchange between the leaf and bulk atmosphere represents the key

to plant water use and photosynthesis (Vialet-Chabrand *et al.*, 2017). Transpiration, stomatal conductance and photosynthesis are intrinsically linked gas exchange processes, all contributing to the dynamics of biomass production and accumulation (Tardieu, 2003). Improving yield under drought is therefore the optimized trade-off between water use and assimilation through stomatal control mechanisms.

The second criterion of Richards (1996) for improving plant yield under drought is early flowering. This response is mostly a temporary escape, although positive associations between plasticity of yield and flowering time across different levels of water availability have been reported (Sadras *et al.*, 2009). In soybean (*Glycine max* (L.) Merr.) most branch growth occurs between initial flowering and the beginning of seed fill, so when drought stress (DS) occurs in this period total seed yield decreases primarily due to a reduction in branch vegetative growth, which reduces branch seed number and branch seed yield (Frederick *et al.*, 2001).

The third criterion for improving plant yield under DS is early leaf area development (Richards, 1996). The leaf area index (LAI) and leaf arrangements through the plant canopy strongly affect light interception (Sinoquet *et al.*, 2000) and leaf photosynthesis (Sarlikioti *et al.*, 2011). Some species also show complex daily heliotropic adjustments of leaf angle. Heliotropism is a reversible morphological characteristic of foliar movements in response to the direct rays of the sun. Mature leaves are critical for the induction and maintenance of heliotropic leaf movements (Vandenbrink *et al.*, 2014).

The ecophysiological significance of heliotropism is related to plant and canopy processes. Paraheliotropism, movements that avoid direct sunlight, can reduce transpiration losses by diminishing light interception, and thus can reduce the negative effects of DS (Kao and Forseth, 1992). Diaheliotropism, movements that track the sun's rays, can increase diurnal carbon gain in canopies with a low LAI (Ehleringer and Hammond, 1987) and reduce carbon gain in canopies with a high LAI (Rakocevic *et al.*, 2010).

Recent studies of heliotropic phenomena have considered the plant–environment interface in three-dimensional (3D) space, simulating soybean mitigation of the effects of UVB (Bawhey *et al.*, 2003). Virtual 3D plants can be used to estimate diverse plant–environment interactions (Godin and Sinoquet, 2005). Movement of the 3D plant architecture by plant functions, such as canopy photosynthesis, is usually based on mechanistic models (Song *et al.*, 2013) called functional–structural plant modeling (Vos *et al.*, 2010). Simulation results suggest that manipulation of stem height, leaf width and leaf angle in rice can optimize plant and canopy photosynthesis (Song *et al.*, 2013). Simulated photosynthetic rates are sensitive to individual plant organ distribution (Song *et al.*, 2013), light and the parameters of enzyme kinetics in photosynthesis-driving processes such as the maximum rate of carboxylation (V_{cmax}) and the potential rate of electron transport (J_{max}) (Walker *et al.*, 2014).

Methods of conventional breeding and marker-assisted selection are being used to develop plant genotypes with better tolerance of DS (Mir *et al.*, 2012). Due to the central role of DREB/CBF transcription factors in abiotic stress responses and their ability to regulate many target 'stress-responsive' genes, they have become popular in genetic engineering aimed at improving abiotic stress tolerance to drought, salt and cold in various plant species. DREB1A was shown to play a role in promoting the expression of drought-tolerance genes in some field crops, for example rice (Dubouzet *et al.*, 2003), bread wheat (Pellegrineschi *et al.*, 2004), tobacco (Kasuga *et al.*, 2004) and soybean (Fuganti-Pagliarini *et al.*, 2017). Greenhouse data comparing DREB1A soybean plants under DS and well-watered conditions suggest that the higher survival rates seen in DS DREB1A plants are due to lower water use and transpiration rates (Polizel *et al.*, 2011).

Ecophysiological models calculate quantitative phenotypic traits (e.g. transpiration rate, organ size and organ expansion rate or biomass accumulation) from environmental inputs such as temperature, light irradiance or soil water potential (Tardieu and Simonneau, 1998). In such models, differences between genotypes are expressed by variations in the parameters of response curves (Tardieu, 2003). It was hypothesized that the DREB1A soybean isoline P58 would show better tolerance to DS than the parental cultivar BR 16 with regard to gas exchange and production traits. Our aim was to follow the central and lateral leaflet movements in vegetative stages V7–V10 and reproductive stages R4–R5 and, using 3D modeling, to integrate those reversible morphogenetic changes into an estimation of daily plant photosynthesis and analyze the distribution of production parameters in BR 16 and its DREB1A isoline P58.

RESULTS

Leaf gas exchange

The central idea of gas exchange measurements was to analyze the absolute and relative modifications of two genotypes in response to water stress. Under non-limiting water conditions (NL), the leaf assimilation (*A*) responses in stages V7–V10 and R4–R5 of two genotypes, BR 16 (Figure 1a,c, respectively) and P58 (Figure 1b,d, respectively), varied sinusoidally through the daily cycle. A slight reduction in leaf *A* at midday and during the early afternoon was perceived (Figure 1, Table 1a). The usual second higher afternoon peak occurred at 14:00–15:00 h in V7–V10 (Figure 1a,b) and at 17:00 in R4–R5 (Figure 1c,d). The absolute

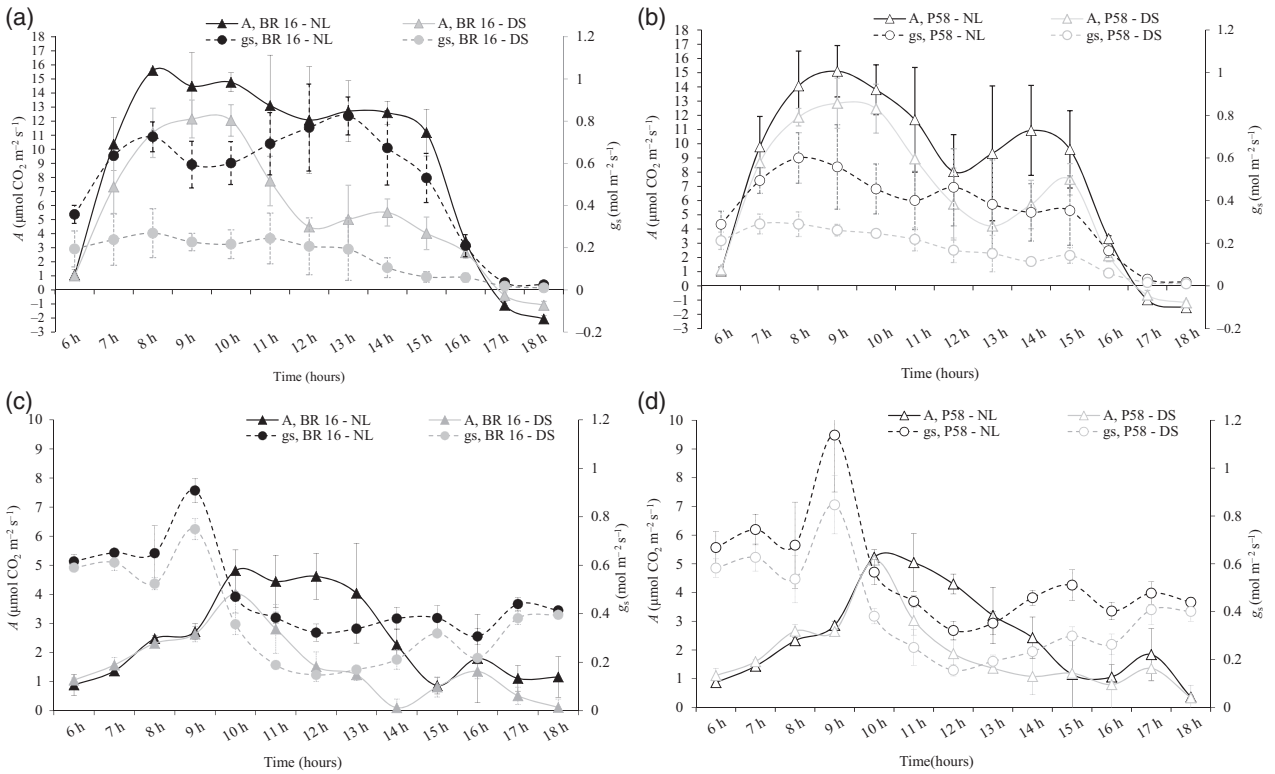

Figure 1. Mean and standard error values ($n = 3$) for leaf net photosynthesis (A, μmol CO_2 m^{-2} sec^{-1}) and stomatal conductance (g_s, mol m^{-2} sec^{-1}) under non-limiting water (NL) and drought-stressed (DS) conditions.
Daily courses were followed in soybean genotype BR 16 for stages (a) V7–V10 and (c) R4–R5 and in its genetically modified isoline BR 16 for stages (b) V7–V10 and (d) R4–R5.

values of A were much larger in the vegetative stages, up to 18 μmol CO_2 m^{-2} sec^{-1} (Figure 1a,b) compared with R4–R5 (Figure 1c,d), when the maximum value was about 6 μmol CO_2 m^{-2} sec^{-1}. The genotype did not influence A in the observed stages (Table 1a), but the water treatment had a strong impact over the daily course, especially at midday and during the early afternoon (Figure 1).

During stages V7–V10 the stomatal conductance (g_s) in BR 16 grown under NL was lower in the morning than in the early afternoon, which allowed a high A to be maintained even in the afternoon (Figure 1a). Under NL, P58 showed a lower g_s (Figure 1b) than BR 16 (Figure 1a) over the daily course in stages V7–V10 (Table 1). In stages R4–R5, P58 had a slightly higher g_s than BR 16 (Table 1, Figure 1c,d). Both genotypes showed similar daily g_s curves, characterized by higher values in the morning (08:00–10:00 h) and strongly reduced values in the afternoon (12:00–18:00 h). Compared with the A curves, the daily curves for g_s in R4–R5 were characterized by early elevation in the morning (10:00–13:00 h) and later reduction (at 14:00–18:00 h).

Both soybean genotypes significantly reduced leaf A and g_s in response to water-limiting conditions (Figure 1, Table 1a). Stronger reductions in A and g_s were noted in BR 16 (41.9% and 63%, respectively) than in P58 (27.3% and 49%, respectively) during stages V7–V10 (Table 1b). In stages R4–R5 stages the relative reduction of A was about 48% in both genotypes, but g_s was reduced slightly more in P58 than in BR 16 (30% compared with 26%, respectively) (Table 1b).

The response to DS was a significantly diminished leaf transpiration rate (E) in both genotypes and all observed stages (Table 1a, Figure 2b). At V7–V10 under NL, E reached its maximum at about 13:00 h and decreased thereafter in BR 16, while in P58 the maximum E values were attained at about 11:00 h and maintained up to 15:00 h (Figure 2a). Under DS, E was lower in P58 than in BR 16 at midday (Table 1a, Figure 2a), inducing a lower relative reduction in E in the genetically modified (GM) isoline than in BR 16 in the vegetative stages (45.9% and 33.2%, respectively) (Table 1b). In R4–R5, E was high over the whole daily cycle (Figure 2b).

Values of WUE were fourfold higher in V7–V10 (Figure 2c) than in R4–R5 (Figure 2d). They varied with genotype, water supply and over the daily course (Table 1a). In V7–V10, the highest WUE was obtained under DS in BR 16 and the lowest were calculated under NL in BR 16 (Figure 2c). In R4–R5, the highest WUE was calculated under

Table 1 ANOVA effects for (a) leaf gas exchange parameters (*A*, leaf photosynthesis; g_s, stomatal conductance; *E*, transpiration; WUE, water-use efficiency) and (b) differences in leaf gas exchange between water-stressed and control treatments over a daily light period in stages V7–V10 and R4–R5 of soybean cultivar BR 16 and its genetically modified isoline P58 cultivated under drought-stress (DS) and non-limiting water conditions (n = 3)*.

	Stages V7–V10				Stages R4–R5			
Variables	*A*	g_s	*E*	WUE	*A*	g_s	*E*	WUE
(a) ANOVA effects for gas exchange*								
Genotype	0.7722	**0.0119**	0.4474	0.2028	0.5782	**0.0954**	**0.0112**	0.5963
Water treatment	**0.0013**	**<0.0001**	**<0.0001**	**<0.0001**	**0.0023**	**<0.0001**	**<0.0001**	0.2949
Time (hours)	**<0.0001**	**<0.0001**	0.3556	**<0.0001**	**0.0004**	**<0.0001**	**<0.0001**	**<0.0001**
Genotype × water	0.3179	**0.0043**	0.1386	**0.0873**	0.4887	0.4052	0.5204	0.2343
Genotype × Time (hours)	0.9432	0.976	0.8234	0.9880	0.9048	0.8095	0.7359	0.8303
Water × Time (hours)	0.8343	0.0606	0.5153	**0.0809**	0.3116	0.7148	0.1677	0.3241
Genotype × water × Time (hours)	0.8943	0.7798	0.8343	0.9876	0.7617	0.8848	0.7964	0.5877
(b) ANOVA effects for gas exchange reduction/increase under DS*								
Genotype	**0.0017**	**0.0077**	**0.0032**	**0.0490**	0.9730	**0.0462**	0.2368	**0.0820**
Time (hours)	**0.0007**	0.3496	**0.0462**	0.9637	**0.0003**	**<0.0001**	**<0.0001**	**0.0039**
Genotype × Time (hours)	0.5975	0.9382	0.7350	0.3436	0.9995	0.2038	0.6732	0.1632

*$P < 0.1$ was considered significant and is indicated in bold type.

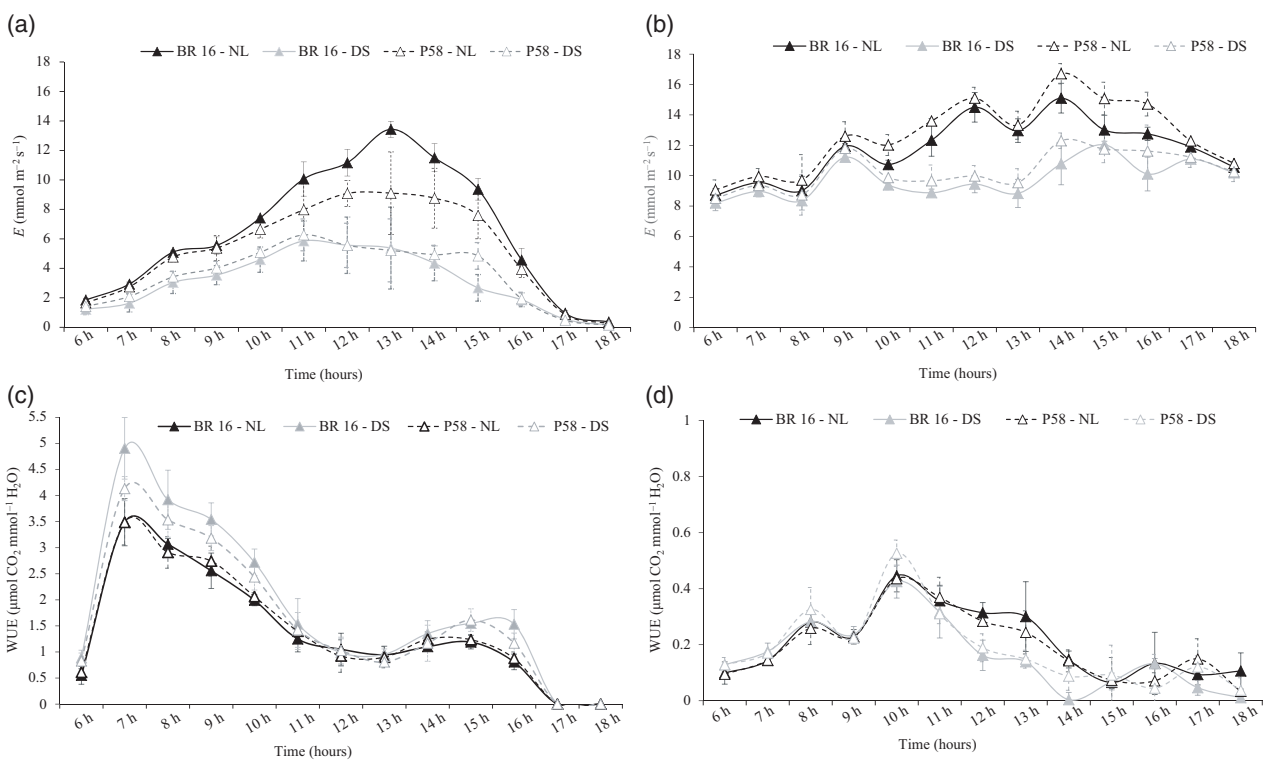

Figure 2. Mean and standard error values (n = 3) of leaf transpiration rate (*E*, mol H_2O m^{-2} sec^{-1}) and water-use efficiency (WUE, µmol $mmol^{-1}$).
Daily courses were followed in the genetically modified isoline P58 of soybean genotype BR 16 cultivated under non-limiting water (NL) and drought-stressed (DS) conditions. Transpiration rate in stages (a) V7–V10 and (b) R4–R5; WUE in stages (c) V7–V10 and (d) R4–R5.

NL in BR 16 and the lowest was calculated under DS in BR 16 (Figure 2d, Table 1a). No significant increase or decrease in WUE under DS was calculated for P58, unlike the significant relative modifications for BR 16 in the vegetative and reproductive stages (Table 2b).

Heliotropic movements

Predominant paraheliotropic movements in both genotypes at two observed stages (Figures 3 and 4) illustrated the basic tendency of daily heliotropic movements of

Table 2 Effects of genotype and water treatments (non-limiting water condition, NL; drought-stressed, DS) on vegetative characteristics, yield parameters, and distribution of filled and abortive pods over the vertical soybean plant profile (low, middle and upper strata) and order of production (main stem, first order; branches, second order) at harvest time: (a) mean ± standard error (SE) of vegetative and yield parameters for $n = 10$; (b) *P*-values according to ANOVA effects of genotype and water treatments*; (c) mean ± standard error (SE) of pods per stratum†; and (d) ANOVA *P*-value for general impacts of stratum and order on pod distribution ($n = 10$).

Genotype	Water treatment	Height (cm)	Metamer Number	Grain	Filled pods	Abortive pods	Aboveground Dry weight (g)	Grain	Filled pods	Abortive pods
(a) Mean ± SE of vegetative and yield parameters										
BR 16	NL	45.5 ± 2.5	11.7 ± 0.4	112.5 ± 13.2	58.2 ± 3.4	9.3 ± 3.1	10.7 ± 0.9	17.6 ± 0.8	27.9 ± 1.0	0.75 ± 0.20
	DS	38.0 ± 1.8	10.1 ± 0.2	65.3 ± 2.5	31.0 ± 1.5	1.2 ± 0.6	3.9 ± 0.3	11.2 ± 0.7	17.8 ± 0.4	0.12 ± 0.03
P58	NL	39.3 ± 1.9	11.8 ± 0.4	130.5 ± 10.0	62.1 ± 4.8	14.8 ± 4.3	10.6 ± 1.5	15.2 ± 1.6	26.3 ± 0.8	0.61 ± 0.19
	DS	38.7 ± 2.5	13.2 ± 0.8	73.9 ± 2.8	36.1 ± 1.5	4.7 ± 1.6	6.4 ± 1.5	10.7 ± 0.3	16.5 ± 0.5	0.37 ± 0.11
(b) ANOVA *P*-values*										
Genotype		0.1985	**0.0032**	0.8225	0.1397	**0.0965**	0.2509	0.1147	0.1398	0.8218
Water treatment		**0.0642**	0.8414	**<0.0001**	**<0.0001**	**0.0014**	**<0.0001**	**<0.0001**	**<0.0001**	**0.0021**
Genotype × water		0.1150	**0.0053**	**0.0855**	0.8415	0.7068	0.2083	0.3177	0.8663	0.2707

Genotype	Treatment	Filled pods Firt order	Filled pods Second order	Abortive pods First order	Abortive pods Second order
(c) Mean ± SE†					
Low stratum					
BR 16	NL	2.6 ± 0.8 a	13.8 ± 2.7 b	0.7 ± 0.4 a	2.0 ± 0.6 b
	DS	1.0 ± 0.4 b	10.1 ± 1.0 b	0.2 ± 0.1 b	0.4 ± 0.2 c
P58	NL	3.4 ± 0.9 a	22.1 ± 3.2 a	1.1 ± 0.4 a	7.4 ± 2.8 a
	DS	0.4 ± 0.3 b	10.9 ± 1.6 b	0.1 ± 0.1 b	2.3 ± 0.8 b
Middle stratum					
BR 16	NL	8.0 ± 1.9 a	16.7 ± 1.8 a	2.0 ± 0.8 a	3.3 ± 1.7 a
	DS	5.1 ± 0.9 b	7.1 ± 1.3 b	0.3 ± 0.3 b	0.3 ± 0.2 b
P58	NL	4.8 ± 0.7 b	16.8 ± 1.8 a	1.8 ± 0.6 a	2.8 ± 1.3 a
	DS	4.4 ± 0.9 b	10.0 ± 1.7 b	0.3 ± 0.2 b	0.8 ± 0.4 b
Upper stratum					
BR 16	NL	11.6 ± 1.1 a	5.5 ± 1.2 a	1.0 ± 0.5 a	0.3 ± 0.2 b
	DS	6.1 ± 0.8 b	1.6 ± 0.3 b	0.0 ± 0.0 b	0.0 ± 0.0 b
P58	NL	10.5 ± 1.3 a	4.5 ± 1.4 a	1.0 ± 0.3 a	0.7 ± 0.2 a
	DS	8.1 ± 0.9 b	2.3 ± 0.8 b	0.6 ± 0.4 b	0.6 ± 0.3 a

Filled pods			Abortive pods		
Stratum	Order	Stratum × order	Stratum	Order	Stratum × order
(d) ANOVA *P*-values*					
<0.0001	**<0.0001**	**<0.0001**	**0.0030**	**0.0012**	**0.0015**

†Averages followed by the same lowercase letter (a, b, c) within the same column are not significantly different considering genotype and water treatment, according to the Tukey test.
*$P < 0.1$ was considered significant and is indicated in bold type.

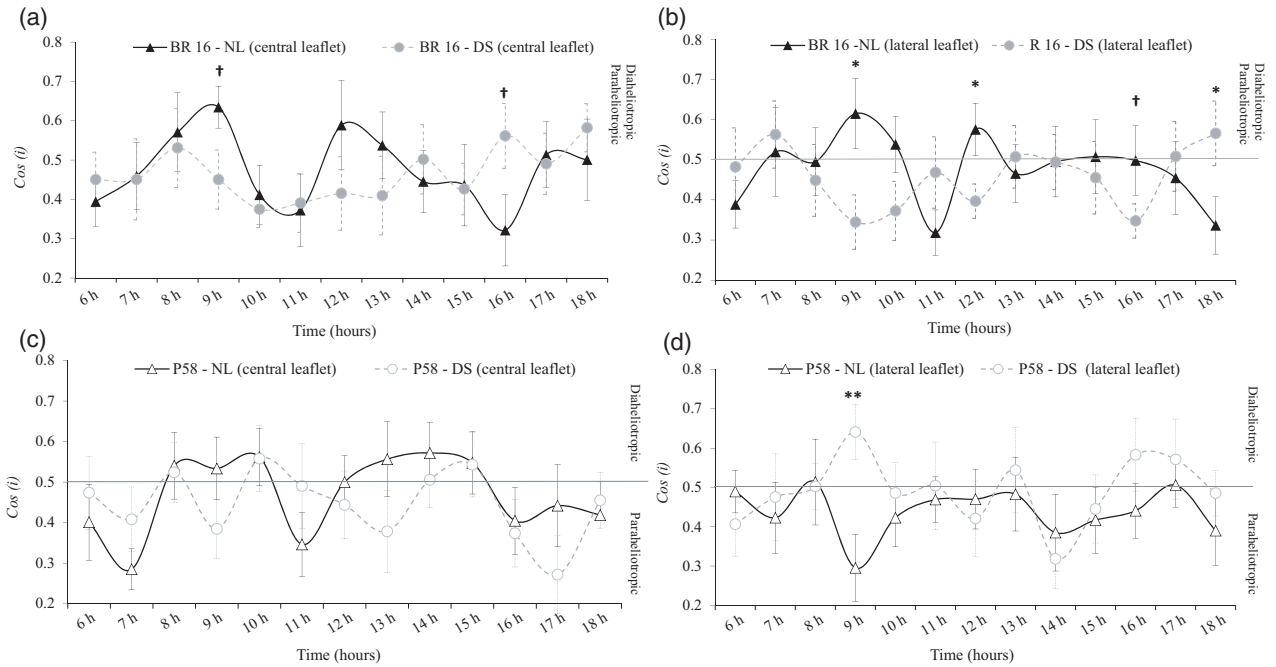

Figure 3. Hourly mean ± standard error for cosine of the angle of incidence, cos *i*, in upper leaves of soybean plants at stages V7–V10 grown under non-limiting water (NL) and drought-stressed (DS) conditions ($n = 10$).
(a) Central and (b) lateral leaflets of BR 16 and (c) central and (d) lateral leaflets of its genetically modified isoline P58. The line for cos $i = 0.5$ is indicated as the division between paraheliotropic and diaheliotropic responses. Levels of statistical significance between water treatments are indicated by: $^{**}P < 0.01$; $^{*}P < 0.05$; $^{\dagger}P < 0.1$.

central and lateral leaflets of upper leaves. Thus, we searched for daily hours characterized by diaheliotropic leaflet positions.

In stages V7–V10, the central and lateral leaflets of BR 16 under NL were characterized by two diaheliotropic movements, at about 09:00 h and 12:00 h, statistically differing from DS (Figure 3a,b). Under DS, the central leaflets showed one diaheliotropic peak at about 16:00 h (Figure 3a) and lateral leaflets had one diaheliotropic movement at the end of daylight (Figure 3b), all statistically different from NL. The central and lateral leaflets of BR 16 showed less numerous diaheliotropic movements under DS than under NL in stages V7–V10.

Under NL, the central leaflets of stage V7–V10 P58 exhibited six daily periods of diaheliotropic movements, from 08:00–10:00 h and from 13:00–15:00 h, which were not statistically different from that seen under DS (Figure 3c). The lateral leaflets of P58 under DS at V7–V10 showed one diaheliotropic movement at 09:00 h and two in the afternoon (16:00 and 17:00 h), while under NL conditions paraheliotropic movements were exclusively expressed (Figure 3d). In this stage, P58 showed more diaheliotropic peaks of lateral leaflets under DS than under NL conditions.

In R4–R5 plants, the central leaflets of BR 16 under NL showed various diaheliotropic movements at 06:00, 08:00, 10:00, 12:00 and 15:00 h, while under DS only one diaheliotropic leaflet position was expressed in the early morning (Figure 4a). The lateral leaflets of BR 16 in R4–R5 plants showed five diaheliotropic movements, at 07:00, 08:00, 13:00, 14:00 and 16:00 h under NL conditions, while under DS these movements were only expressed at 08:00, 10:00 and 14:00 h (Figure 4b). The daily behavior of BR 16 in stages R4–R5 was like that in stages V7–V10, expressing fewer diaheliotropic movements of central leaflets under DS than under NL conditions.

At stages R4–R5 the central leaflets of P58 showed slight diaheliotropic movements – under NL at 07:00 and 17:00 h and under DS at 06:00 and 15:00 h (Figure 4c). The lateral leaflets of P58 at stages R4–R5 under NL exhibited four diaheliotropic movements (06:00, 10:00, 12:00 and 17:00 h), while under DS they showed five diaheliotropic peaks (07:00, 09:00, 11:00, 12:00 and 16:00 h) (Figure 4d). This daily heliotropic pattern of lateral leaflets in R4–R5 was like that expressed in stages V7–V10 (Figure 3d), but with more diaheliotropic movements of lateral leaflets in P58 under DS than under NL.

Vegetative and yield parameters

Drought had a significant impact on all observed final vegetative and reproductive features (Table 2a). It significantly reduced the final stem height in both genotypes, showing a

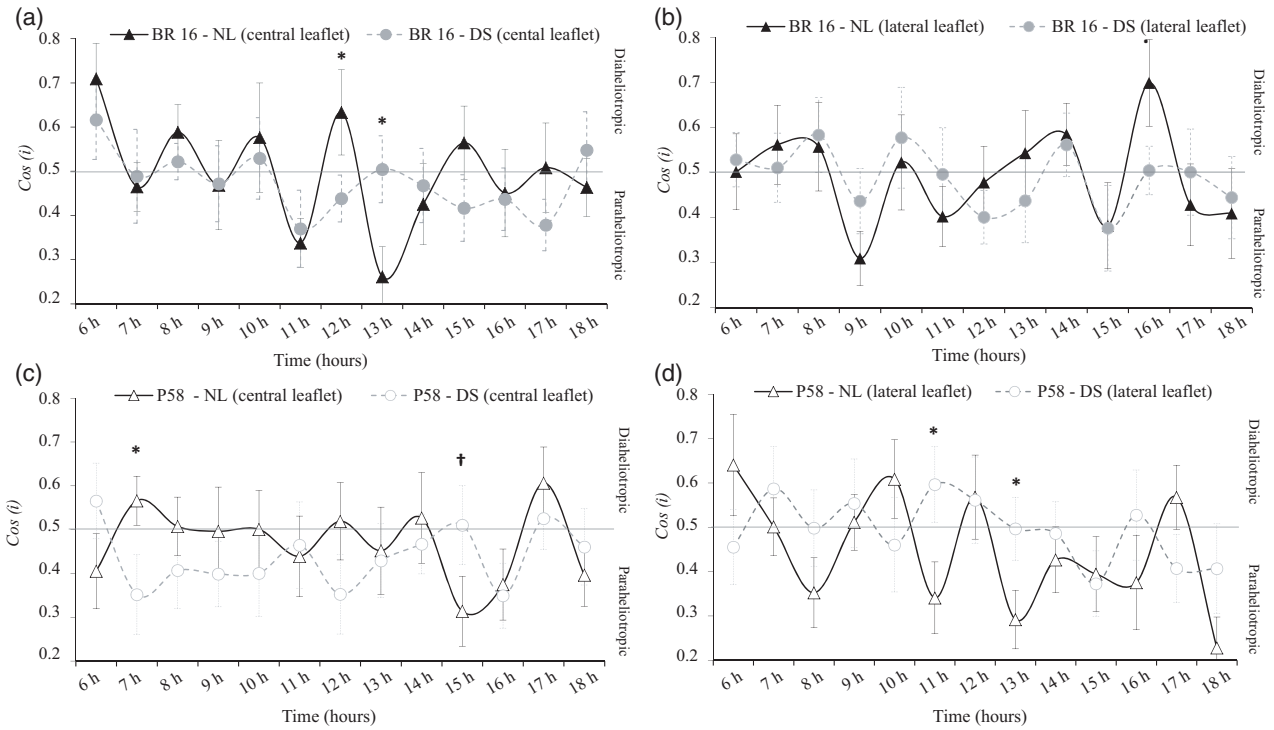

Figure 4. Hourly mean ± standard error for the cosine of the angle of incidence, *cos i*, in the upper leaves of soybean plants at stages R4–R5 grown under non-limiting water (NL) and drought-stressed (DS) conditions (n = 10).
(a) Central and (b) lateral leaflets of BR 16 and (c) central and (d) lateral leaflets of its genetically modified isoline P58. The line for cos i = 0.5 is indicated as the division between paraheliotropic and diaheliotropic responses. Levels of statistical significance between water treatments are indicated by: $^{*}P < 0.05$; $^{\dagger}P < 0.1$.

higher impact in BR 16 than in P58, but having a similar effect on reduction of aboveground vegetative dry matter (DM).

The impact of genotype was observed on main stem metamer number under DS (Table 2a,b). Metamer number decreased in BR 16 and increased in P58 under DS. The number of abortive pods was significantly higher in P58 than in BR 16. On the other hand, the DM of abortive pods did not differ between genotypes.

The observed yield parameters, as grain DM or DM of filled and abortive pods, were strongly reduced under DS compared with NL (Tables 2a and 2b). The grain number diminished in both genotypes under DS; grain number per plant was not significantly different between genotypes under NL but was significantly lower in BR 16 than in P58 under DS.

The number of filled and abortive pods over two axis orders (main stem first-order axis and branches second-order axis) observed over three strata of the vertical plant profile (low, middle, upper) varied significantly (Table 2c, d). The number of filled pods on the main stem was significantly lower than on relative branching structures in low and middle strata (Table 2d). The opposite situation between order axes was observed in the upper stratum, where the branching structure carried a smaller number of filled pods than the main stem. The production of filled pods increased gradually over the main stem from low to upper strata and decreased over the branching structure from low and middle strata to the top of the plants. The distribution of abortive pods on first-order axes showed a decrease from low and middle strata to the upper stratum, while on second-order axes the highest number was found in the low plant stratum, especially in the P58 genotype.

The impact of DS was evident in the final number of filled and abortive pods, considering originating axis order and vertical profile (Table 2c). The impact of genotype was less evident. In the low stratum plants under NL produced roughly double the number of filled pods in P58 than in BR 16 on second-order axes (Table 2d). No difference in the number of filled pods on second-order axes in the low stratum was observed in BR 16 plants grown under NL compared with DS conditions. In the middle stratum under NL a higher number of filled pods were produced in BR 16 than in P58. No difference in the number of filled pods on the main stem in the middle stratum was observed in P58 plants grown under NL and DS. The number of abortive pods on second-order axes in the low and upper strata was significantly higher in P58 than in BR 16.

Estimations of plant photosynthesis over daylight periods

The mock-ups were processed by dividing the daylight into four distinct periods, based on the general heliotropic responses of the upper leaves (Figures 3 and 4). The first

period corresponded to the early morning (06:00–07:00 h) characterized by prevalent paraheliotropic movements of central and lateral leaflets, with the exception of the central leaflets of P58 under NL in stages R4–R5 (Figure 4c). The second morning period (08:00–10:00 h) considered the opposite positions among lateral leaflets in P58 and BR 16 in stages V7–V10 (Figure 3b,c); when some avoided direct sunlight the others moved in a diaheliotropic sense. In the third daylight period (11:00–15:00 h), both types of leaflets showed the same significant diaheliotropic peaks, about 12:00 h for stages V7–V10 (Figure 3b) and at 11:00, 12:00, 13:00 and 15:00 h for stages R4–R5 (Figure 4a,c,d). During the remaining hours of the third daily period, the heliotropic movements were predominantly neutral. The fourth daylight period occurred during late afternoon (16:00–18:00 h) and was characterized by diaheliotropic movements at 16:00 h occurring in two observed stages in both leaflet types and for two water treatments (Figures 3a,b and 4b,c) and one at 18:00 h in stages V7–V10.

The estimated photosynthesis of the central leaflet (A') was obtained by compiling mock-ups in VegeSTAR for four daily periods in trees (Figure S3) and comparing the estimations with measured values of A, considering stages V7–V10 and R4–R5 (Figure 1a,c, respectively). The estimated A' for central leaflets was slightly reduced compared with A, judging by the bias of −0.065 (Figure S3), and was well adjusted, considering the low dispersion (RMSE = 1.016).

The well-adjusted estimations at leaf scale (Figure S3) allowed daily estimations of plant photosynthesis (A_p, μmol CO_2 plant^{-1} sec^{-1}) for the entire daylight period (Figure 5). There were four scenarios for the same soybean plant leaf area (LA), each having different leaflet positions. Soybean mock-ups were compiled for stages V7–V10 (Figure 5a) and R4–R5 (Figure 5b).

Leaf area was not modified after short-term drought in V7–V10 (Figure 5a) but after long-time exposure in R4–R5 water limitation significantly reduced LA (Figure 5b). In the

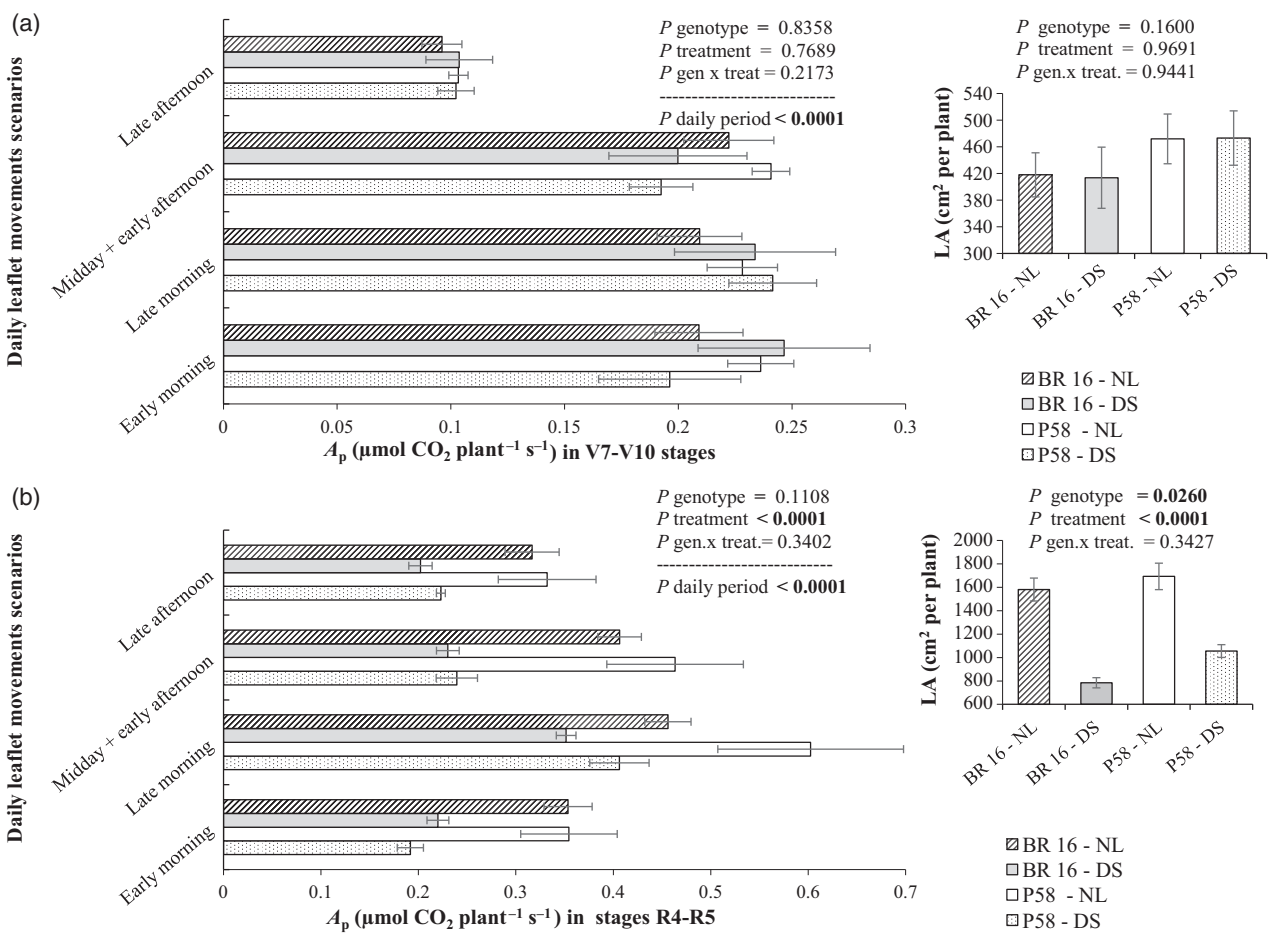

Figure 5. Mean ± standard error values (n = 3) of estimated average leaf area (LA) and daily plant photosynthesis (A_p, μmol CO_2 plant^{-1} s^{-1}).
(a) Stages V7–V10 and (b) stages R4–R5. Four daily scenarios and the respective mock-ups were computed for whole day period. Soybean cultivar BR 16 and its genetically modified isoline P58 were cultivated under non-limiting water (NL) and drought-stressed (DS) conditions . ANOVA P-values for the effects of genotype, water treatments and daily period were calculated. $P < 0.1$ was considered significant and is given in bold type.

reproductive stages, the GM isoline P58 formed a higher LA than BR 16, especially under DS (Figure 5b).

The modifications in leaflet positions over the course of the day resulted in different values of A_p (*P*-value for daily period <0.0001; Figure 5). The general late afternoon leaflet positions avoiding direct sunlight led to a significant reduction in A_p compared with other scenarios in stages V7–V10 and R4–R5 (Figure 5a). In R4–R5 a significant reduction of A_p was also observed in the early morning scenario (Figure 5b). In V7–V10, the estimated A_p was not affected by water availability or genotype (Figure 5a) in all plant scenarios. In R4–R5 water limitation had an effect on the significant reduction of estimated A_p in both BR 16 and P58 in all scenarios tested (Figure 5b).

DISCUSSION

Heliotropic movements in soybean

All soybean species are members of the Fabaceae family, characterized by diverse types of leaf movements. The site of light perception for leaf movements in Fabaceae is located at the pulvinus. The mechanism of movement is similar to that of guard cells (Lee *et al.*, 2014), led by an asymmetric turgor gradient formed between the adaxial and abaxial motor cells (Satter *et al.*, 1974). Potassium ion influx coupled with chlorine ions is powered by a proton gradient that results in osmotic influx. In Fabaceae, oxalate crystals that occur only in endodermal cells of the pulvinus help to produce slow movements, while starch grains always present in endodermal cells of the pulvinus correlate with all kinds of movements (Rodrigues and Machado, 2007).

Heliotropic movements occur under well-watered conditions but also under water stress, and are modified by perception of light, temperature and water vapor conductance in the pulvinus (Fu and Ehleringer, 1989). Since under the same external conditions the two studied genotypes differed in their patterns of heliotropic movements, it is possible that differences in genotype in their pulvinar regions gave rise to distinct perceptions and/or responses. The pattern of daily movements of BR 16 central leaflets in stages V7–V10 and R4–R5 were similar, with fewer diaheliotropic movements under DS than under NL. However, the lateral leaflets in stages V7–V10 and R4–R5 showed more diaheliotropic movement in DS P58 plants than in plants grown under NL. The prevalence of diaheliotropic movements in lateral leaflets of drought-tolerant GM P58 under stress might be due to mechanisms triggered under DS by the transcription factor DREB1A; by binding at the DRE region on promoters of target genes it can induce defense responses. In the GM line P58, drought-response genes including *GmPI-PLC* (phospholipase C), *GmSTP* (sorbitol transporter protein), *GmGRP* (glycine-rich RNA-binding protein) and *GmLEA14* (late embryogenesis abundant) are highly expressed under DS in the greenhouse (Polizel *et al.*, 2011). Under DS in field conditions, phosphatase *GmPP2C* (Glyma14 g195200), a gene related to stomatal closure, alanine aminotransferase *GmAlaAT* (Glyma01 g026700 and Glyma07 g045900), a protein evolved in nitrogen metabolism, 1-1-pyrroline-5-carboxylate synthetase (P5CS; Glyma18 g034300) and a putative soybean aquaporin pip1/UDPgalactose transporter (Glyma12 g066800), proteins involved in osmotic adjustment under DS, are expressed more in P58 than in BR 16 (Fuganti-Pagliarini *et al.*, 2017). Such a genetic background enables P58 plants to get rid of excess light resulting from higher absorption in diaheliotropic central leaflet movements.

The heliotropic responses of glass-greenhouse grown V7–V10 and R4–R5 BR 16 plants were very similar to those cultivated under field conditions in low (V4–V6) and of high (R5) LAI stages (Rakocevic *et al.*, 2010). Similar responses at more advanced vegetative stages can be attributed to the fact that plants in glass-greenhouse pots were physically less densely distributed and experienced less competition for light than in field conditions. On the other hand, the values of cos *i* defining diaheliotropic movements were lower in glass-greenhouse than in field research conditions (Rakocevic *et al.*, 2010). This could be explained by the light modifications under glass-greenhouse conditions, because heliotropic leaf movements are induced by blue light (Koller, 1986). Glass reduces photomorphogenetically active blue light by about 7% (McMahon *et al.*, 1990); however, even though reduced, leaf movements are still induced in the glass-greenhouse experiment.

Gas exchange responses and heliotropic movements

The leaf *A* and WUE experienced slight reduction during midday hours, as a consequence of general plant responses to high light incidence and temperature. It seems that due to high light intensity and high temperatures at midday the pulvinus is already oriented to its ultimate extreme inducing a paraheliotropic response (Raeini-Sarjaz and Chalavi, 2008). The sinusoidal daily cyclic response of *A* is a typical response of soybean cultivars (Ehleringer and Hammond, 1987). The second afternoon higher peak in *A*, which occurred at about 14:00–15:00 h in V7–V10 and at about 17:00 h in R4–R5, also occurs in various soybean genotypes under field conditions (Turner *et al.*, 1978).

The central and lateral leaflets of BR 16 under NL manifested the response described for soybean (Rosa *et al.*, 1991), namely diaheliotropism in the early morning and in the late afternoon when light intensity and air temperature were lower and paraheliotropism at noon when light intensity and temperature are higher. The morning diaheliotropic movements were probably due to optimization of

carbon gain during the most intensive diurnal assimilation period in soybean grown under NL, while the afternoon diaheliotropic response was probably related to the second peak in photosynthesis. On the other hand, the predominant paraheliotropism of central and lateral leaflets in V7–V10 and R4–R5 indicated a strategy for escaping DS. Paraheliotropism, a plant feature that avoids photoinhibition by reducing light interception, affects the capacity to maintain high CO_2 assimilation rates throughout the day in well-watered bean plants (Pastenes *et al.*, 2005).

In V7–V10, the central leaflets of P58 cultivated under DS showed 4-h periods of diaheliotropism. This sun-tracking behavior of the central leaflets of P58 compensated for the reduction in diaheliotropic movements of the lateral leaflets. In R4–R5 fewer diaheliotropic movements were observed in the central leaflets of P58 under DS than under NL. Paraheliotropic movements and a reduced LA (accumulated carbon gain invested in leaves) under DS compared with NL could be responsible for the lower A_p of both genotypes at this stage. Integrating key processes at the plant scale permits predictions of multiscale photosynthesis and carbon partitioning (Weston *et al.*, 2012). In our study, the integration of A_p additionally included daily modifications of plant structure. Photosynthesis by itself does not play any direct role in the perception of vectorial excitation of heliotropic movements (Fu and Ehleringer, 1989). Significant correlations between leaf incident angles and leaf A have been reported (Rosa *et al.*, 1991; Raeini-Sarjaz and Chalavi, 2008), helping us to understand why plants can improve their photosynthetic performance with paraheliotropic leaf movements (Bielenberg *et al.*, 2003) that relieve the risk of photoinhibition (Zhu *et al.*, 2015).

The most sensitive gas exchange parameter in the responses of the two genotypes to water stress was g_s. In V7–V10 g_s was lower in P58 than in BR 16, while in the reproductive stages the situation was reversed. Normally, paraheliotropic leaves have greater A and g_s, leading to greater daily transpiration (Habermann *et al.*, 2011), as was expressed in our experiment, especially in BR 16 in V7–V10. Under water-limiting conditions, E at midday was lower in P58 than in BR 16, giving a lower relative reduction in E in P58 than in BR 16 in the vegetative stages.

For genotypic comparisons, WUE and the harvest index are drivers of yield (Blum, 2009). A non-significant relative increase in WUE was calculated for P58 at V7–V10 under water stress, which together with the lower relative reduction in E indicates better drought tolerance in P58 than in BR 16. This physiological behavior of P58 plants had already been observed in the greenhouse (Polizel *et al.*, 2011) and in two different field experiments conducted during the 2011/2012 (Rolla *et al.*, 2014) and 2013/2014 (Fuganti-Pagliarini *et al.*, 2017) crop seasons. The adaptive significance of heliotropic movements leads to better water use in *Capparis spinosa* (Levizou and Kyparissis, 2016). The adaptive significance of paraheliotropism is mostly related to the promotion of carbon assimilation by increasing light-use efficiency rather than enhancing photoprotection (Habermann *et al.*, 2011). Heliotropic movements of leaflets in soybean suggest that improvement of photosynthesis, g_s, dissipation of excess light energy as a photoprotective mechanism and better WUE are strategies to improve soybean performance.

Heliotropic movements related to architectural and productive characteristics

Drought significantly reduced all observed final vegetative and reproductive architectural features. Final stem height, reduction in aboveground vegetative DM, metamer number and grain number per plant were less sensitive to DS conditions in P58 than in BR 16.

Among the productive features on second-order axes, the soybean plants cultivated under NL conditions produced roughly double the number of filled pods in P58 than in BR 16. The number of abortive pods on second-order axes in the low and upper layers was significantly higher in P58 than in BR 16 (mainly the effect of genotype), but this resulted in a similar total final DM in both genotypes. This was caused by the lower weight of individual abortive pods in P58 than in BR 16, meaning that there was similar investment of carbon in a relatively greater number of abortive pods in P58. Such a strategy in P58 could be used to reduce the eventual final loss, by aborting a high number of pods and achieving the maximum possible grain production in continued DS conditions. This means that P58 could have a 'decision strategy' depending on continuation of drought, maintaining the possibility of producing more pods and grains if drought ends during the seed-filling stage. This strategy, related to second Richards criterion (Richards, 1996), could be tested in the field, because in nature the occurrence of rainfall during the pod-filling stage is always possible, permitting even greater expression of AtDREB1A.

In a previous analysis in crop season 2011/2012, DREB1A soybean plants did not outperform BR 16 in terms of yield under field conditions but showed superiority in the number of seeds and total number of pods when stress was applied in the vegetative stages (Rolla *et al.*, 2014). In crop season 2013/2014, when a severe drought was registered, P58 plants also had a higher number of pods per plant than BR 16 and exhibited a final yield of 1.938 kg ha^{-1} in non-irrigated conditions, greater than the 1.868 kg ha^{-1} of BR 16 (Fuganti-Pagliarini *et al.*, 2017). Overexpression of AtDREB1A in soybean appears to slightly enhance drought tolerance in stages V7–V10 and R4–R5 and could be indirectly related to fine reversible leaflet movements, improving leaf and plant CO_2 assimilation, LA and distribution of pod production in the plant, thus improving yield.

Our experiment showed the three main criteria for improving the yield potential (biomass) in drought environments (Richards, 1996; Bhatia *et al.*, 2014) were better optimization of transpiration, WUE and formation of a higher LA per plant after long-term DS in the P58 GM isoline than in parental BR 16. An approach linking these physiological traits to empirical breeding for yield could increase the probability of crosses resulting in additive gene action for drought adaptation, and a more thorough characterization of the germplasm would permit more globalized strategies in plant responses to stress (Bhatia *et al.*, 2014). Under DS in the vegetative stages P58 showed compensation of prevalent paraheliotropic tendencies in central leaflet movements by diaheliotropic positions of lateral leaflets. This genotype manifested relatively lower reductions in A and g_s than BR 16 under DS, followed by an insignificant increase in WUE and lower relative reduction in E, which together lead to a higher capacity to maintain the water status. Leaf gas exchange, architectural and productive features together indicate higher drought tolerance in the GM isoline than in BR 16.

Finally we stress that the genetically engineered isoline P58 was less drought sensitive than the parental BR 16. DREB1A could be involved in various responses to DS, from alleviating its impacts through the high frequency of paraheliotropic movements of central leaflets and the higher frequency of diaheliotropic movements of lateral leaflets, to lower transpiration, fine-tuning of WUE and g_s, higher LA and abortion of pods to achieve the possible maximum grain production under continuous DS conditions.

EXPERIMENTAL PROCEDURES

Plants, micro-climate and drought treatment descriptions

The drought-sensitive Brazilian soybean cultivar BR 16 (Oya *et al.*, 2004) was transformed by particle bombardment (Rech *et al.*, 2008) with rd29A:AtDREB1A at the Embrapa Soybean Plant Biotechnology Laboratory (Polizel *et al.*, 2011). The obtained plants underwent molecular analysis. The best construct-positive line (P58), containing rd29A:AtDREB1A, was selected (Stolf-Moreira *et al.*, 2011) and multiplied for further investigation.

The GM line P58 at the T_6 generation and the parental BR 16 were seeded on 2 October 2009 (one plant per pot containing about 3250 ml of sand). Plants were cultivated in a glass-greenhouse at Embrapa Soybean, Londrina (23°11′ S, 51°10′ W, elevation 612 m), Paraná, Brazil.

The treatments included two genotypes (BR 16 and P58) and two water treatments (NL and DS). A completely randomized design with 10 replications for each treatment was applied. From 9 November 2009 to harvesting on 2 February 2010, soil gravimetric humidity was set to and maintained at 15–19% (near to field capacity) and 5–7.6%, by weighing the pots twice a day and supplementing with water or nutrient solution as needed, following the procedure for moderate to high soybean water restriction (Casagrande *et al.*, 2001). All pots received 50 ml of balanced nutrient solution (pH 6.6) twice a week.

Gas exchange measurements

Leaf gas exchange (A, net photosynthetic rate, μmol CO_2 m^{-2} sec^{-1}; g_s, stomatal conductance, mol m^{-2} sec^{-1}; E, transpiration rate, mmol H_2O m^{-2} sec^{-1}) were measured at the central leaflet of the most recently produced fully expanded leaf in three representative plants for each treatment, using a portable photosynthesis system (LI-6400). Leaf gas exchange parameters were recorded every hour and performed twice during plant development on two particular dates corresponding to stages V7–V10 (11 November 2009) and R4–R5 (14 December 2009). The WUE was calculated as A/E (Medrano *et al.*, 2015). The daily course of temperature and photosynthetic photon flux density at the upper leaf level is given in Figure S1 in the online Supporting Information. Relative reduction or relative increase in gas exchange and WUE under the water treatments were calculated as the percentage of each individual value under one water treatment in relation to the other.

Plant codification for mock-ups reconstructions

Both BR 16 and P58 soybean genotypes are of the determinate growth type, and their leaves are characterized as multiform leaves (Champagne *et al.*, 2007). The first stem metamer has two cotyledonal leaves opposite each other. The second stem metamer has two unifoliate leaves opposite each other and phyllotaxy of 90° in relation to the cotyledons. Production of adult trifoliate leaves starts at the third metamer, initiated in spiral phyllotaxy.

All 40 pots with soybean plants were marked, indicating the orientation of cotyledons and the first trifoliate leaves to the north, at stage V5, to help 3D reconstructions in space under the VPlants methodology (Pradal *et al.*, 2009). The codification in multiscale tree-graphs (MTGs) (Godin and Caraglio, 1998) was performed from the bottom to the top of the plants, which allowed the development of the same plants to be followed in three stages: (i) V7–V10 on 10–13 November 2009; (ii) R4–R5 on 14–16 December 2009; (iii) harvest on 2 February 2010. Stages (i) and (ii) also corresponded to leaf gas exchange measurements.

The coding was performed at three scales of decomposition ('/'): (i) plant (P), (ii) axes (G) and (iii) metamers (C, F, E and D) (Figure S2). The axis scale of decomposition was used to codify: the main stem of the first branching order; the second and third branching ('+') order axes; and the long main leaf petioles, permitting the inclusion of their length. At the metamer scale several features were differentiated: (i) two small opposite aboveground cotyledons (C), (ii) juvenile metamer with the first pair of single leaves with opposite phyllotaxy (F), (iii) branch metamers (following one after the other, i.e. $E1 < E2 \ll En$), (iv) trifoliate metamer of the main long petiole (E1) bearing two lateral leaflets assumed to be of equal size and (v) the central metamer of the trifoliate leaf composed of the short petiole (D1) bearing a central leaflet. The plant MTGs contained the following information: length of each metamer, length and width of leaflets, differentiating information between the central leaflet and the lateral ones, length of long (E1) and short petioles (D1), inclination of axes and petioles. The attributed virtual phyllotaxy of spirally arranged trifoliate leaves was 170° to avoid overlay, and the branching followed the same phyllotaxy rules. We codified the number of flowers and initiated pods in R4–R5, and the number of filled and empty pods after harvest.

To compute the impact of heliotropic movements on an hourly scale, the central and lateral leaflet movements were reconstructed by modification of the angles of elevation (α) and rotation (β) in the MTG. Each leaflet object was constructed from 16

triangles. The mock-ups were visualized in PlantGLViewer (Pradal *et al.*, 2009), and exported to VegeSTAR, software that allows the calculation of leaf area and computing light interception and photosynthesis (Adam *et al.*, 2006).

Distribution of vegetative and yield parameters

The final main stem height, DM of grains per plant, DM of filled pods per plant, DM of empty pods per plant and DM of stems and leaves were measured after harvest ($n = 10$). The main stem height measurements and main stem length from MTGs served for general validation of plant size. The distribution of pods was calculated on a scale of axes (main stem and branches), three strata of vertical profile (low, middle and upper) and whole plants. The numbers of filled and empty pods per metamer of the main stem and per branch as the number of pods per layer were extracted from MTGs with use of AMAPStudio (Griffon and de Coligny, 2014).

Heliotropic leaflet movements in soybean

Heliotropic movements were monitored in 10 plants for each treatment, on the same dates when leaf gas exchange measurements were performed. Leaf elevation and azimuth were measured on the central leaflet of the most recent fully expanded leaf. Leaflet position was defined by the cosine of the angle of incidence (cos *i*), which is the cosine of the angle between a normal to the sun's direct rays and the leaflet lamina (Prichard and Forseth, 1988). This expresses the proportion of the direct beam that is incident on the leaflet. Therefore, a cos *i* of 1 describes a leaflet with its adaxial surface perpendicular to the direct beam, a value of −1 denotes a leaflet with its abaxial surface perpendicular to the direct beam (diaheliotropic position), while a value of 0 represents a leaflet which is parallel to the direct solar beam (paraheliotropic position). The cos *i* was calculated using the equation of Prichard and Forseth, 1988:

$$\cos i = \cos\beta \cdot \cos z + sin\beta \cdot sinz \cdot \cos(a_s - a_l) \quad (1)$$

where β is the leaflet angle from the horizontal, z is the solar zenith angle, a_s is the solar azimuth angle and a_l is the leaf azimuth.

The measurements were performed using the methodology developed by Rakocevic *et al.* (2010), estimating the leaflet angles from digital images of each plant taken horizontally and azimuthally every hour. Digital image shots were taken during a 1-day cycle from 06:00 to 18:00 h under settings that took 1040 pictures in each of 2 days, representing stages V7–V10 and R4–R5. The first image was taken from 'above' (camera pointing vertically down, to measure a_l) and the second one was taken 'sideways' from north to south (camera pointing horizontally, to measure β).

The leaflet angles registered in the digital images were determined in the laboratory using GIMP 2.8 software. For a_l south is 0°, east is −90°, west is +90° and north is −180 or +180° (Ehleringer and Hammond, 1987). The solar angles were computed using the software VegeSTAR. The resulting daily sequence files contained data on solar angle for each minute computed for two dates of observation for the coordinates of Londrina-PR, Brazil.

Integration of photosynthesis at the plant scale

The estimation of leaf photosynthesis by VegeSTAR software is based on Farquhar's model (Farquhar *et al.*, 1980), and the software allows the integration of photosynthesis at the plant scale. To compute light interception and photosynthesis VegeSTAR requires information about the environment (azimuth and height of the sun, global radiation, diffuse radiation, air temperature and air [CO_2]). The variation in physical and meteorological parameters during the two specific dates representing stages V7–V10 and R4–R5 were taken from micro-environmental measurements (irradiance and temperature) or computed by VegeSTAR (azimuth and height of the sun). V_{cmax}, J_{max} and dark respiration (R_d) are also necessary for the estimation of photosynthesis at leaf and plant scales using VegeSTAR (Adam *et al.*, 2006). For simulations we used values of R_d from light curves of BR 16 and the DREB isoline (Table S1), and modeled V_{cmax} and J_{max} (Gilbert *et al.*, 2011).

The simulated rate of leaf photosynthesis (A', μmol CO_2 m^{-2} sec^{-1}) was first adjusted to the measured values of A for each of the four daily periods defined by heliotropic movements (see Results), in three representative plants of two genotypes under two water availability treatments in which the leaf photosynthesis was measured. Validation was done using the following procedure: (i) the mock-ups of representative plants were 'fixed' in their heliotropic movements at four particular times (07:00, 09:00, 13:00 and 16:00 h) representing four daylight periods defined after data analyses (see Results); (ii) for each of the four daily periods in V7–V10 and R4–R5 a sequence demanded by VegeSTAR software was built, varying the physical and meteorological parameters over 10-min intervals; (iii) R_d, V_{cmax} and J_{max} varied between DS and NL conditions, stages, daylight periods and genotypes (Table S1), approximating the outputs to the measured A values; other parameters of the implemented VegeSTAR equations were used as software default values; (iv) the measured central leaflets of the upper leaves were identified in the VegeSTAR output, which contained the computed LA and its relative A' for each of 16 triangles of each leaflet that comprised the soybean foliage; (v) the mean A' value for 16 triangles comprising a virtual central leaflet was used for comparison with measured A.

Once A' was validated, A_p (plant photosynthesis) was calculated as the integration considering leaf area (m^2) of each leaf triangle and its A'. A_p was computed for the whole daylight period from 06:00 to 18:00 h following a daily sequence. Four forms of each plant (scenarios) were considering for the four daylight periods of divergence in heliotropic responses.

Statistical analyses

Statistical analyses were performed with the R language and software (2017). ANOVA 'lme' and 'lm' functions were applied to test the significance of genotype, water availability treatment and hour of the daily cycle associated with leaf gas exchange, cos *i* and mean leaf photosynthesis per plant for vegetative and reproductive parameters. When the 'lme' function was used, the plant replication was used as a random factor. The Tukey test was applied to analyze the impact of genotype and water treatments on the number of filled and abortive pods in each stratum and axis order that supported pods. The package 'qpcR' was used for RMSE calculation. The ANOVA *P*-values are shown in tables following the respective figures, or as significance codes for cos *i*.

ACKNOWLEDGEMENTS

MR acknowledges Brazilian Foundations Araucária and Consórcio Pesquisa Café for invited researcher fellowships. We thank Claudinei de Freitas Toledo for technical support.

CONFLICT OF INTEREST

The authors declare no conflict of interest.

SUPPORTING INFORMATION

Additional Supporting Information may be found in the online version of this article.

Figure S1. Daily courses of photosynthetic active radiation and temperature in the glass-greenhouse corresponding to stages V7–V10 and R4–R5.

Figure S2. Illustration of soybean plant coding.

Figure S3. Comparison between the measured net photosynthesis and estimated values for central leaflets in stages V7–V10 and R4–R5.

Table S1. V_{cmax}, J_{max} and R_d applied in scenarios for estimating A_p for stages V7–V10 and R4–R5 stages.

REFERENCES

Adam, B., Dones, N. and Sinoquet, H. (2006) VegeSTAR: software qui calcule l'interception lumineuse et la photosynthèse, version 3.2: INRA.

Bawhey, C., Grant, R.H. and Wei, G. (2003) Digital measurement of heliotropic leaf response in soybean cultivars and leaf exposure to solar UVB radiation. *Agric. For. Meteorol.* **120**, 161–175. https://doi.org/10.1016/j.agrformet.2003.08.013.

Bhatia, V.S., Jumrani, K. and Pandey, G.P. (2014) Developing drought tolerance in soybean using physiological approaches. *Soybean Res.* **12**, 1–19.

Bielenberg, D.G., Miller, J.D. and Berg, V.S. (2003) Paraheliotropism in two *Phaseolus* species: combined effects of photon flux density and pulvinus temperature, and consequences for leaf gas exchange. *Environ. Exp. Bot.* **49**, 95–105. https://doi.org/10.1016/S0098-8472(02)00062-X.

Blum, A. (2009) Effective use of water (EUW) and not water-use efficiency (WUE) is the target of crop yield improvement under drought stress. *Field Crops Res.* **112**, 119–123. https://doi.org/10.1016/j.fcr.2009.03.009.

Casagrande, E.C., Farias, J.R.B., Neumaier, N., Oya, T., Pedroso, J., Martins, P.K., Breton, M.C. and Nepomuceno, A.L. (2001) Expressão gênica diferencial durante déficit hídrico em soja. *R. Bras. Fisiol. Veg.* **13**(2), 168–184. https://doi.org/10.1590/S0103-31312001000200006.

Champagne, C.E.M., Goliber, T.E., Wojciechowski, M.F., Mei, R.W., Townsley, B.T., Wang, K., Paz, M.M., Geeta, R. and Sinha, N.R. (2007) Compound leaf development and evolution in the legumes. *Plant Cell.* **19**, 3369–3378. https://doi.org/10.1105/tpc.107.052886.

Cook, I.B., Smerdon, J.E., Seager, R. and Coats, S. (2014) Global warming and 21st century drying. *Clim. Dyn.* **43**, 2607–2627. https://doi.org/10.1007/s00382-014-2075-y.

Dubouzet, J.G., Sakuma, Y., Ito, Y., Kasuga, M., Dubouzet, E.G., Miura, S., Seki, M., Shinozaki, K. and Yamaguchi-Shinozaki, K. (2003) OsDREB genes in rice, *Oryza sativa* L., encode transcription activators that function in drought-, high-salt- and cold-esponsive gene expression. *Plant J.* **33**, 751–763. https://doi.org/10.1046/j.1365-313x.2003.01661.x

Ehleringer, J.R. and Hammond, S.D. (1987) Solar tracking and photosynthesis in cotton leaves. *Agric. For. Meteorol.* **39**, 25–35. https://doi.org/10.1016/0168-1923(87)90013-X.

Farquhar, G.D., von Caemmerer, S. and Berry, J.A. (1980) A biochemical model of photosynthetic CO_2 assimilation in leaves of C3 species. *Planta*, **149**, 78–90. https://doi.org/10.1007/BF00386231.

Frederick, J.R., Camp, C.R. and Bauer, P.J. (2001) Drought-stress effects on branch and mainstem seed yield and yield components of determinate soybean. *Crop Sci.* **41**, 759–763. https://doi.org/10.2135/cropsci2001.413759x.

Fu, Q.A. and Ehleringer, J.R. (1989) Heliotropic leaf movements in common beans controlled by air temperature. *Plant Physiol.* **91**, 1162–1167. https://doi.org/10.1104/pp.91.3.1162.

Fuganti-Pagliarini, R., Ferreira, L.C., Rodrigues, F.A. *et al.* (2017) Characterization of soybean genetically modified for drought tolerance in field conditions. *Front. Plant Sci.* **8**, 448. https://doi.org/10.3389/fpls.2017.00448.

Gilbert, M.E., Zwieniecki, M.A. and Holbrook, N.M. (2011) Independent variation in photosynthetic capacity and stomatal conductance leads to differences in intrinsic water use efficiency in 11 soybean genotypes before and during mild drought. *J. Exp. Bot.* **62**(8), 2875–2887. https://doi.org/10.1093/jxb/erq461.

Gobarah, M.E., Tawfik, M.M., Thalooth, A.T. and El-Housini, E.A. (2015) Water conservation practices in agriculture to cope with water scarcity. *Int. J. Water Res. Arid Environ.* **4**, 20–29.

Godin, C. and Caraglio, Y. (1998) A multiscale model of plant topological structures. *J. Theor. Biol.* **191**, 1–46. https://doi.org/10.1006/jtbi.1997.0561.

Godin, C. and Sinoquet, H. (2005) Functional-structural plant modelling. *New Phytol.* **166**, 705–708. https://doi.org/10.1111/j.1469-8137.2005.01445.x.

Griffon, S. and de Coligny, F. (2014) AMAPstudio: an editing and simulation software suite for plants architecture modeling. *Ecol. Modell.* **290**, 3–10. https://doi.org/10.1016/j.ecolmodel.2013.10.037.

Habermann, G., Ellsworth, P.F.V., Cazoto, J.L., Feistler, A.M., da Silva, L., Donatti, D.A. and Machado, S.R. (2011) Leaf paraheliotropism in *Styrax camporum* confers increased light use efficiency and advantageous photosynthetic responses rather than photoprotection. *Environ. Exp. Bot.* **71**, 10–17. https://doi.org/10.1016/j.envexpbot.2010.10.012.

Kao, W.Y. and Forseth, I.N. (1992) Diurnal leaf movement, chlorophyll fluorescence and carbon assimilation in soybean grown under different nitrogen and water availability. *Plant, Cell Environ.* **15**, 703–710. https://doi.org/10.1111/j.1365-3040.1992.tb01012.x.

Kasuga, M., Miura, S., Shinozaki, K. and Yamaguchi-Shinozaki, K. (2004) A combination of the *Arabidopsis* DREB1A gene and stress-inducible rd29A promoter improved drought and low-temperature stress tolerance in tobacco by gene transfer. *Plant Cell Physiol.* **45**, 346–350 PMID: 15047884.

Koller, D. (1986) The control of leaf orientation by light. *Photochem. Photobiol.* **44**, 819–826. https://doi.org/10.1111/j.1751-1097.1986.tb05542.x.

Lee, H., Garrett, W.M., Sullivan, J., Forseth, I. and Natarajan, S.S. (2014) Proteomic analysis of the pulvinus, a heliotropic tissue, in *Glycine Max*. *Int. J. Plant Biol.* **5**(1), https://doi.org/10.4081/pb.2014.4887.

Levizou, E. and Kyparissis, A. (2016) A novel pattern of leaf movement: the case of *Capparis spinosa* L. *Tree Physiol.* **36**, 1117–1126. https://doi.org/10.1093/treephys/tpw059.

McMahon, M.J., Kelly, J.W. and Decoteau, D.R. (1990) Spectral transmittance of selected greenhouse construction and nursery shading material. *J. Environ. Hortic.* **8**, 118–121.

Medrano, H., Tomás, M., Martorell, S., Flexas, J., Hernández, E., Rosselló, J., Pou, A., Escalona, J.-M. and Bota, J. (2015) From leaf to whole-plant water use efficiency (WUE) in complex canopies: limitations of leaf WUE as a selection target. *Crop J.* **3**(3), 220–228. https://doi.org/10.1016/j.cj.2015.04.002.

Mir, R.R., Zaman-Allah, M., Sreenivasulu, N., Trethowan, R. and Varshney, R.K. (2012) Integrated genomics, physiology and breeding approaches for improving drought tolerance in crops. *Theor. Appl. Genet.* **125**, 625–645. https://doi.org/10.1007/s00122-012-1904-9.

Oya, T., Nepomuceno, A.L., Neumaier, N., Farias, J.R.B., Tobita, S. and Ito, O. (2004) Drought tolerance characteristics of the Brazilian soybean cultivars. Evaluation and characterization of drought tolerance among Brazilian soybean cultivars in the field. *Plant Prod. Sci.* **7**, 129–139. https://doi.org/10.1626/pps.7.129.

Pastenes, C., Pimentel, P. and Lillo, J. (2005) Leaf movements and photoinhibition in relation to water stress in field-grown beans. Leaf movements and photoinhibition in relation to water stress in field-grown beans. *J. Exp. Bot.* **56**, 425–433. https://doi.org/10.1093/jxb/eri061.

Pellegrineschi, A., Reynolds, M., Pacheco, M., Brito, R.M., Almeraya, R., Yamaguchi-Shinozaki, K. and Hoisington, D. (2004) Stress-induced expression in wheat of the *Arabidopsis thaliana* DREB1A gene delays drought-stress symptoms under greenhouse conditions. *Genome*, **47**, 493–500. https://doi.org/10.1139/g03-140.

Polizel, A.M., Medri, M.E., Nakashima, K. *et al.* (2011) Molecular, anatomical and physiological properties of a genetically modified soybean line transformed with rd29A:AtDREB1A for the improvement of drought tolerance. *Genet. Mol. Res.* **10**(4), 3641–3656. https://doi.org/10.4238/2011.

Pradal, C., Boudon, F., Nouguier, C., Chopard, J. and Godin, C. (2009) PlantGL: a Python-based geometric library for 3D plant modelling at different scales. *Graph. Models*, **71**, 1–21. https://doi.org/10.1016/j.gmod.2008.10.001.

Prichard, J.M. and Forseth, I.N. (1988) Photosynthetic responses of two heliotropic legumes from contrasting habitats. *Plant, Cell Environ.* **11**, 591–601. https://doi.org/10.1111/j.1365-3040.1988.tb01801.x.

R Development Core Team. (2017) *R: a language and environment for statistical computing*. Vienna, Austria: R Foundation for Statistical Computing. Available at: https://www.R-project.org/

Raeini-Sarjaz, M. and Chalavi, V. (2008) Pulvinus activity, leaf movement and leaf water-use efficiency of bush bean (*Phaseplus vulgaris* L.) in a hot environment. *Int. J. Biometeorol.* **52**, 815–822. https://doi.org/10.1007/s00484-008-0175-2.

Rakocevic, M., Neumaier, N., Oliveira, G.M., Nepomuceno, A.L. and Farias, J.R.B. (2010) Heliotropic responses of soybean cultivars at three phenological stages and under two water regimes. *Pesq. Agropec. Bras.* **45**, 661–670. https://doi.org/10.1590/S0100-204X2010000700005.

Rech, F.L., Vianna, G.R. and Aragão, F.J.L. (2008) High-efficiency transformation by biolistics of soybean, common bean and cotton transgenic plants. *Nat. Protoc.* **3**, 410–418. https://doi.org/10.1038/nprot.2008.9.

Richards, R.A. (1996) Defining selection criteria to improve yield under drought-stress. *Plant Growth Regul.* **20**, 157–166. https://doi.org/10.1007/BF00024012.

Rodrigues, T.M. and Machado, S.R. (2007) The pulvinus endodermal cells and their relation to leaf movement in legumes of the Brazilian cerrado. *Plant Biol.* **9**, 467–477.

Rolla, A.A.P., Carvalho, J.F.C., Fuganti-Pagliarini, R. *et al.* (2014) Phenotyping soybean plants transformed with rd29A:AtDREB1A for drought tolerance in the greenhouse and field. *Transgenic Res.* **23**(1), 75–87. 1007/s11248-013-9723-6

Rosa, L.M., Dillenburg, L.R. and Forseth, I.N. (1991) Responses of soybean leaf angle, photosynthesis and stomatal conductance to leaf and soil water potential. *Ann. Bot.* **67**, 51–58. https://doi.org/10.1093/oxfordjournals.aob.a088099.

Sadras, V.O., Reynolds, M.P., de la Veja, A.J., Petrie, P.R. and Robinson, R. (2009) Phenotypic plasticity of yield and phenology in wheat, sunflower and grapevine. *Field Crops Res.* **110**, 242–250. https://doi.org/10.1016/j.fcr.2008.09.004.

Sarlikioti, V., de Visser, P.H.B., Buck-Sorlin, G.H. and Marcelis, L.F.M. (2011) How plant architecture affects light absorption and photosynthesis in tomato: towards an ideotype for plant architecture using a functional-structural plant model. *Ann. Bot.* **108**, 1065–1073. https://doi.org/10.1093/aob/mcr221.

Satter, R.L., Applewhite, P.B. and Galston, A.W. (1974) Rhythmic potassium flux in *Albizzia* - Effect of aminophylline, cations, and inhibitors of respiration and protein-synthesis. *Plant Physiol.* **54**, 280–285.

Sinoquet, H., Rakocevic, M. and Varlet-Grancher, C. (2000) Comparison of models for daily light partitioning in multispecies canopies. *Agric. For. Meteorol.* **101**, 251–263. https://doi.org/10.1016/S0168-1923(99), 00172-0.

Song, Q., Zhang, G. and Zhu, X.-G. (2013) Optimal crop canopy architecture to maximize canopy photosynthetic CO_2 uptake under elevated CO_2 - a theoretical study using a mechanistic model of canopy photosynthesis. *Funct. Plant Biol.* **40**, 109–124. https://doi.org/10.1071/FP12056.

Stolf-Moreira, R., Lemos, E.G.M., Carareto-Alves, L. *et al.* (2011) Transcriptional profiles of roots of different soybean genotypes subjected to drought stress. *Plant Mol. Biol. Rep.* **29**, 19–34. https://doi.org/10.1007/s11105-010-0203-3.

Tardieu, F. (2003) Virtual plants: modelling as a tool for the genomics of tolerance to water deficit. *Trends Plant Sci.* **8**, 9–14.

Tardieu, F. and Simonneau, T. (1998) Variability among species of stomatal control under fluctuating soil water status and evaporative demand. Modelling isohydric and anisohydric behaviors. *J. Exp. Bot.* **49**, 419–432. https://doi.org/10.1093/jxb/49.Special_Issue. 419.

Tuberosa, R. (2012) Phenotyping for drought tolerance of crops in the genomics era. *Front. Physiol.* **3**, 1–26. https://doi.org/10.3389/fphys.2012.00347.

Turner, N.C., Begg, J.E., Rawson, H.M., English, S.D. and Hearn, A.B. (1978) Agronomic and physiological responses of soybean and sorghum crops to water deficits. III. Components of leaf water potential, leaf conductance, $^{14}CO_2$ photosynthesis, and adaptation to water deficits. *Aust. J. Plant Physiol.* **5**, 179–194. https://doi.org/10.1071/PP9780179.

Vandenbrink, J.P., Brown, E.A., Harmer, S.L. and Blackman, B.K. (2014) Turning heads: the biology of solar tracking in sunflower. *Plant Sci.* **224**, 20–26. https://doi.org/10.1016/j.plantsci.2014.04.006.

Vialet-Chabrand, S.R.M., Matthews, J.S.A., McAusland, L., Blatt, M.R., Griffiths, H. and Lawson, T. (2017) Temporal dynamics of stomatal behavior: modeling and implications for photosynthesis and water use. *Plant Physiol.* **174**, 603–613. https://doi.org/10.1104/pp.17.00125.

Vos, J., Evers, J.B., Buck-Sorlin, G.H., Andrieu, B., Chelle, M. and de Visser, P.H.B. (2010) Functional-structural plant modelling: a new versatile tool in crop science. *J. Exp. Bot.* **61**, 2101–2115. https://doi.org/10.1093/jxb/erp345.

Walker, A.P., Beckerman, A.P., Gu, L., Kattge, J., Cernusak, J.A., Domingues, T.F., Scales, J.C., Wohlfahrt, G., Wullschleger, S.D. and Woodward, F.I. (2014) The relationship of leaf photosynthetic traits – *V*cmax and *J*max – to leaf nitrogen, leaf phosphorus, and specific leaf area: a meta-analysis and modeling study. *Ecol. Evol.* **4**, 3218–3235. https://doi.org/10.1002/ece3.1173.

Weston, D.J., Hanson, P.J., Norby, R.J., Tuskan, G.A. and Wullschleger, S.D. (2012) A conceptual model for integrating multi-scale networks. *Plant Signal Behav.* **7**(2), 260–262. https://doi.org/10.4161/psb.18802.

Zhu, C.G., Chen, Y.N., LI, W.H., CHEN, X.L. and HE, G.Z. (2015) Heliotropic leaf movement of *Sophora alopecuroides* L.: an efficient strategy to optimize photochemical performance. *Photosynthetica*, **53**, 231–240. doi.org/10.1007/s11099-015-0089-2